GeoPlanning
Journal of Geomatics and Planning
Vol. 8, No. 1, 2021

e-ISSN: 2355-6544

Received: 13 March 2020;
Accepted: 1 January 2021;
Published: 30 July 2021.

Keywords:
EDM, Refraction, Sensors

*Corresponding author(s) email:
felipe.carvajalro@gmail.com

Original Research Open access

Temperature Acquisition System for Real Time Application of First Velocity Correction by EDM (Electronic Distance Measurement)

Felipe A. C. Rodriguez [1*], Luis A. K. Veiga [1], Wilson A. Soares [1]

1. *Federal University of Paraná*

DOI: 10.14710/geoplanning.8.1.61-74

Abstract

The first velocity correction is used to correct the measured distance affected by the velocity variation of the electromagnetic wave propagation in a medium. This correction depends on the refractive index of the propagation medium and reference refractive index. The influence of the temperature in the medium refractive index is critical; some estimates establish that variation 1°C causes 1ppm of error in distances. In the measuring processes with total stations, the temperature is usually collected at only one point, for example, in the position where the measuring instrument is setup. However, the wave propagates in a medium of non-constant temperature, where the extremes of the line can present variations and thus this measurement in only one point could be non-representative. In this context, it was developed a low-cost real-time temperature acquisition system. This system provides the temperature values in different locations allowing their monitoring through the time. Experiments realized during the geodetic monitoring of a dam, show variations up to 8°C among geodetic points on the dam and around it. An analysis was development to evaluate the influence of temperature variations on monitoring distances and geodetic coordinate of a 2d network with different approaches (temperature modeling). The results shows different values for distances (1.0 mm) and coordinates (0.5 mm) depending of the approach choose.

1. Introduction

The accuracy of the distances obtained by electronic distances measurement (EDM) technique is a critical factor to some applications as geodetic network monitoring or geodetic control of structures (Brunner, 1984; Ussisoo, 1969; Scaioni et al., 2014). The accuracy of EDM depends of two factors; the first, known as internal, is related with the manufacturing characteristics own of each instrument. On second case found the external factors that are more complex since depend mainly of the environmental conditions of the medium in which the electromagnetic wave propagates (Rüeger, 1990). According Brunner (1984); Rüeger (1990); Torge & Müller (2012) and Ogundare (2015) the principal effect that generate the medium is the variation of propagation velocity of the wave due to mainly density changes in their composition. This situation affect directly the distance compute and therefore their accuracy.

According to Brunner (1984), the ideal situation to geodetic calculations it would be when the wave propagated in the vacuum, this supposes a homogeneous and constant medium however, the troposphere, medium of propagation associated to the terrestrial measurements, is constantly changing their composition (density). Rüeger (1990), define that the principal components of the troposphere that change their composition and affect the velocity propagations of wave in EDM instruments are the pressure, humidity and temperature. The correction of the effects which the atmospheric parameters of pressure, humidity and temperature cause on the wave velocity propagation are modeled through the refractive index, this is a factor that related the velocity

of light of propagation in a medium and in the vacuum. For EDM corrections, the refractive index is used to compute the first velocity correction, the last one provide the distance bias generated by the variation of the velocity of the electromagnetic wave due to the medium composition (Rüeger, 1990). The Equation 1 presented the first velocity correction:

$$K = (n_f - n_L) \cdot d \quad (1)$$

Where:

K = the first velocity correction
n_f = the reference refractive index
n_L = group refractive index valid for atmospheric conditions described by t, p, e
d = electronic distance or distance influenced by atmospheric parameters

The refractive index of the medium depends on the frequency of the electromagnetic radiation propagating through it and the composition of the medium. In 1963, The International Union of Geodesy and Geophysics (IUGG) decided, in the XIIIth General Assembly, that the refractive index for light and NIR waves (employed in the electronic distance measurement) could be reduced to ambient conditions through the simplification of the formula proposed by Barrel e Sears 1939 (Rüeger, 1990). The Equation 2 shows how to obtain the refractive index.

$$n_L = 1 + \frac{n_g - 1}{1 + \alpha \cdot t} \cdot \frac{p}{1013.25} - \frac{4.125 \cdot 10^{-8}}{1 + \alpha \cdot t} \cdot e \quad (2)$$

Where:

n_L = group refractive index valid for atmospheric conditions described by t, p, e
n_g= group refractive index
t = dry bulb temperature of air (°C)
p = atmospheric pressure (mb)
α = coefficient of expansion of air (= 0.003661 per °C)
e = partial water vapor pressure (mb)

Other simplification was proposed by Kohlrausch (1955), cited by Rüeger (1990). In this case the coefficient of the air expansion varies slightly doing $\alpha = 1/273.15$. With this modification, through Equation 3 the refractive index is obtained:

$$(n_L - 1) = (n_g - 1) + \frac{273.15 \cdot p}{(273{,}15 + \mathrm{t}) \cdot 1013.25} \cdot \frac{11.27 \cdot 10^{-6}}{(273.5 + \mathrm{t})} \cdot e \quad (3)$$

The error in the refractive index due to pressure, temperature and humidity parameters can be estimated by the partial differentials of the Kohlrausch formulate. In Rüeger (1990) and Ogundare (2015) are presented examples that shows that, for the refractive index of light, the temperature is critical for the determination of the refractive index. According to the authors, for a temperature of 15°C, a pressure of 1007 mb, a partial water vapor pressure of 13 mb and a group refractive index of 1.0003045, a pressure variation of 1.0mb generates an error of 0.3 ppm in the distance determination, humidity variation of 1mb produces 0.04 ppm of error in the distance, meanwhile, the temperature variation of 1°C results in an error of 1ppm in the distance determination.

The measurement of atmospheric parameters is a typical procedure to land surveys engineers before to staring a measurement. Torge & Müller (2012) present gradients of -0.0065°C/m, -0.12hPa/m, -0.0035hPa/m, to temperature, pressure e humidity respectly. From these values is posibile conluding that the temperature presents more variation in function to changes in the altitude. Rüeger (1990) and Angus-Leppan & Brunner (1980), postulate that the average between the measurement of the pressure and humidity parameters at both terminal of a line are sufficient to achieve the representative value, however for the temperature parameter the average is not always representative, since the temperature gradients in the lower atmosphere are unstable. The principal cause for this is the different heat absorption and emission capacities of the Earth's surfaces. In this context Brunner (1984), postulate that the development of instrument solutions to measure the atmospheric parameters can be provide information that permit the modeling of this parameters, therefore obtain a better estimation of refractive index and of the first velocity correction.

Actually, the total stations have a microprocessor to automatic compute of the refractive index and first velocity correction, for this, the user should be to insert the atmospheric values, and the correction is made. In this case, the use of external atmospheric sensors are necessary. In addition, some total stations have internal sensors to measure the atmospheric parameters. For both cases, the measure is made in one place; therefore, this not considered the variations of atmospheric parameters around it, mainly the temperature. The problem of the representative of these values has led to the development of an atmospheric monitoring system as well as estimation models from the data provide by these systems. An example is a sensor development by Solarić et al. (2012), this sensor provides atmospheric data to calculate the atmospheric corrections on the EDM calibration baseline, this system permits measure the data on the each pillar of the baseline. Artese & Perrelli (2018), Proposed a method using the climatic data and a digital terrain model (DTM) of a landslide area, in this case the model is done to entire area. The next step after collected of data, it is the modeling of parameters, in this context Robertson (1977); Brunner & Fraser (1977); Angus-Leppan & Brunner (1980); Fraser (1981) and Brunner & Rüeger (1992), presented mathematical models to atmospheric parameters estimation. To apply each of these models, the measurements of atmospheric parameters are necessary.

Currently, low-cost technology has allowed the development of programmable sensors, microcontrollers like Arduino or Raspberry, communication modules like Xbee or LoRA. In this context, we present a temperature acquisition system to monitoring and collect the temperature data, critical parameter to compute the refraction index. This system was developed through the concept of real time wireless sensor network (RWSN), with open-source hardware and software and low-cost sensors. Two experiment was presented with objective of evaluate the operation of this system and the temperature monitoring, also was presented an example to evaluate the incidence of the variations of this parameter on a 2D topographic network.

2. Data and Methods

For the proposed temperature acquisition system was selected different devices, and in some cases evaluated and configured them as it will be shown later. For the communication, the Zigbee protocol was chosen; through radio frequency Xbee S2C devices, this protocol provides wireless communication. In the case of the control system, the microcontroller Arduino Uno allowed the configuration of parameters used to send data and temperature measurements and with which frequency. Finally, it was evaluated the digital temperature sensor DS18B20 (classic and waterproof version) and the TMP36 analog temperature sensor. This allowed choosing the one that was more suitable for this work. Below each step developed is detailed.

2.1. DS18B20 and TMP36 temperature sensors

The evaluation applied to DS18B20 and TMP36 sensor seeks to choose the more suitable sensor for this work. The TMP36 sensor is analog and provides voltage differences that can be converted in temperature through a scale factor (Devices, 2020). The D18B20 is a digital sensor with two versions; classical, not

encapsulated, and waterproof, both versions provide directly temperature values (Maxim, 2020). The main characteristics are presented in the Table 1.

Table 1. Main characteristics of both sensors.

Sensor	TMP36	DS18B20
Operating system	Analog	Digital
Precision	±2°C	±0,5°C
Operation range	- 40°C to 125°C	- 10°C to 85°C

2.2. Comparison between DS18B20, TMP36 temperature sensors and the standard thermometer

It was compared both DS18B20 (classical version) and TMP36 sensors, related to a standard glass mercury thermometer of 0.1°C nominal precision, defined as the reference of the response in temperature range. This experiment was developed in the physics laboratory at Federal University of Paraná. The experiment consisted in inducing temperature values through a thermostatic bath that permits to heat one solution from the 7°C to 100°C range. Figure 1, shows that the thermometer and sensors were submerged in water.

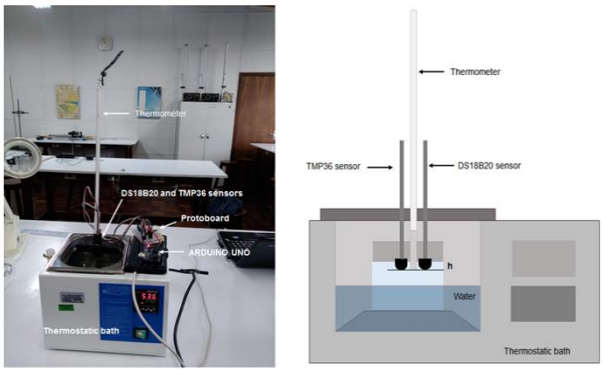

Figure 1. Thermostatic bath and experiment configuration

The circuit shown in Figure 2 is composed by an Arduino Uno microcontroller, DS18B20 and TMP36 sensors, and provides automatically the temperature. The temperature values from the thermometer correspond to analogic measurements.

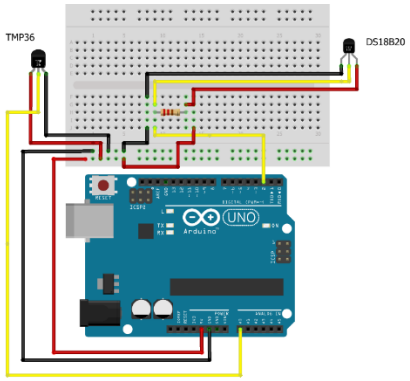

Figure 2. DS18B20 and TMP36 circuit for comparative experiment

The results of this experiment are shown in the Figure 3, in this case it were realized 73 temperature measurements. The approximate range of these values is 10°C to 45° C.

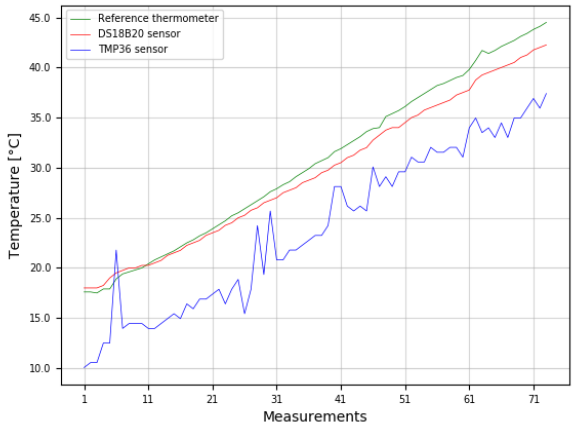

Figure 3. Evolution temperature during of experiment.

For evaluating the differences between temperature series of DS18B20, TMP36 sensors and the reference thermometer, it was used the Pearson's Chi-squared statistical test with a 95% confidence interval (Agresti, 2007). In this case, the expected values (E) correspond to the reading of the glass reference thermometer; the observed values (O) correspond to the measurements of the sensors TMP36, DS18B20, and n correspond to the number of sample elements.

$$\chi^2_{estimated} = \sum_{i}^{n} \frac{(O_i - E_i)^2}{E_i} \tag{4}$$

The degrees of freedom are defined by:

$$v = (r-1) \cdot (k-1) \tag{5}$$

Where:

v: degrees of freedom
r: number of rows
k: number of columns

Two hypotheses were proposed, H0 the samples are homogeneous and H1 the samples are not homogeneous. Table 2 shows the results:

Table 2. The Pearson's Chi-squared statistical test for TMP36 and DS18B20 sensors

Sensor	v	$\chi^2_{estimated}$	$\chi^2_{p-value}$
TMP36	72	114.908	47.857
DS18B20	72	3.488	47.857

Considering the results obtained in the experiment, it is possible to conclude that the better adherence of the results were obtained with the DS18B20 sensor in comparison with the results obtained by the TMP36 sensor, so the hypothesis H_0, for the sensor DS18B20, was accepted, however for the sensor TMP36 it was not. Based on the results obtained in this statistical test it was chosen as the best option for the development of this work the DS18B20 sensor (Soares, 2006; De Rubeis et al., 2017).

2.3. DS18B20 sensor correction

The next step was the calibration of DS18B20 sensor, in this case it was used the waterproof version because this has a more resistant structure. It was applied the same test of the previous experiment. The Figure 4 shown the temperature curve of the DS18B20 sensor and thermometer

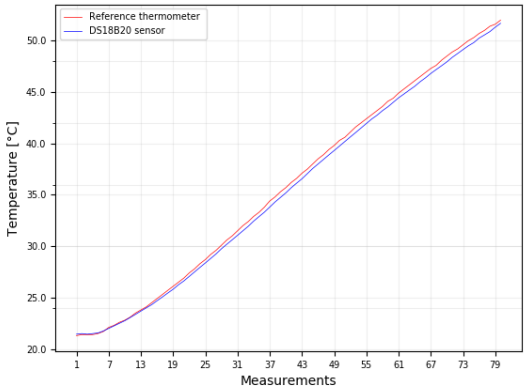

Figure 4. Thermometer and DS18B20 temperature evolution

For this experiment, it was realized 79 temperature measurements. The approximate range of these values is 22 °C to 60°C, maximum thermometer graduation. Two hypotheses were proposed, Ho the samples are homogeneous and H_1 the samples are not homogeneous. Table 3 shown the results:

Table 3. The Pearson's Chi-squared statistical test for DS18B20 waterproof sensor

Sensor	v	$\chi^2_{estimated}$	$\chi^2_{p-value}$
DS18B20	78	0.346	51.910

The Figure 5, shows the temperature difference between DS18B20 sensor and the reference thermometer. In addition, a trend line adjusted by a second-degree polynomial, calculated from difference values between the thermometer and DS18B20 sensor, provides the correction function for temperature sensor measurements, the calibration function is:

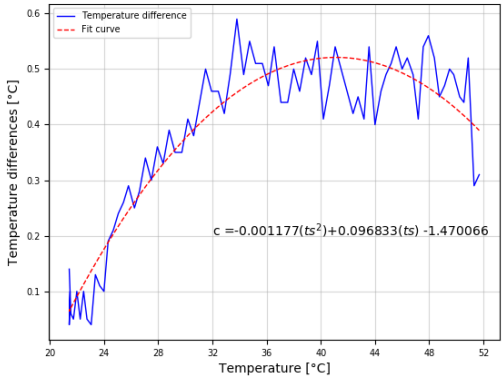

Figure 5. Temperature differences between DS18B20 sensor and thermometer, trend-line and correction function

The estimated temperature for the DS18B20 sensor used is:

$$t_c = t_s + (-0.001177 \cdot {t_s}^2 + 0.096833 \cdot t_s - 1.470066) \quad (6)$$

Where:

t_c=Correction temperature values
t_s= DS18B20 temperature values

2.4. Arduino and Xbee configuration

The Xbee devices were configured with the API (application programming interface) operating mode; this mode is available for the operation of the Zigbee protocol, used in this case, and permits the Xbee coordinator to receive wireless data packets from multiple Xbee devices, identifying each remote device. This characteristic is fundamental to associate each Xbee device with a geographic location. We used the star topology in this Zigbee network, configuring a coordinator and router devices. With an Arduino Uno board, it was possible to control the data to be sent to the network and the temperature measurement frequency, for this, two sketches control the transmission and reception of data in nodes and in coordinator respectively. For those Arduino Uno boards integrated with the remote devices, the format of the data is the principal function since the sensor measurement must be sent as well as its identification. In the case of coordinator, the Arduino Uno board must interpret the data packet received.

The network is composed of five nodes and one coordinator. Each node has a DS18B20 temperature sensor, Xbee S2C module, and an Arduino Uno microcontroller. For the coordinator, the configuration is the same, but the DS18B20 is not used. Figure 6 shows the configuration of the coordinator and the node.

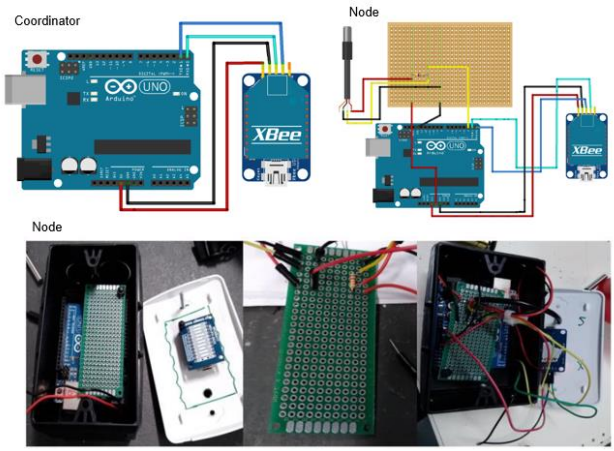

Figure 6. Coordinator and node structure for the wireless network.

For the coordinator, the energy power was provided by the USB port connection. For the nodes, due to their characteristic of being positioned in different positions on the ground, it was used a solar panel-based power and batteries, the latter being used as a reserve, if there are any problems in the power supply from the solar panels. Figure 7 shows the configuration of node energy system

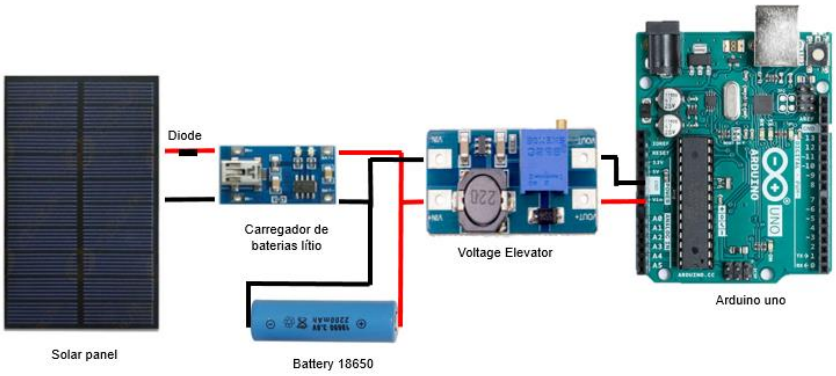

Figure 7. Configuration of node energy system

The configuration of this power source considers a 5.5-volt solar panel, a one-way diode; a lithium battery charger, a lithium battery, and a voltage lift to keep this parameter constant during its use. The node and coordinator are shown in Figure 8.

Figure 8. Coordinator and nodes of network

The upper part of the module has two functions: the first is protecting the temperature sensor from the direct incidence of the sunrays and, secondly, it supports the solar panel. This part can be rotated for better positioning of the solar panel. Figure 9 shows the wireless network diagram, in this case, the nodes were configured to send the temperature values each 1 minute to the coordinator. The coordinator controls the data flow and a sketch in python language save the information

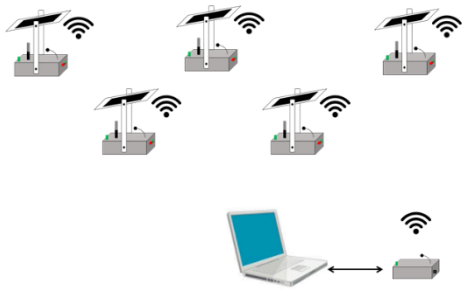

Figure 9. Network operation diagram

The collected temperature data, received by the coordinator node, were transmitted to the computer that was connected to the total station. One program developed in C # language receives this information and, using a user-selected interpolation model, determined the temperature value to be used for the correction of the first velocity. This program automatically sets the temperature and pressure values for the total station.

3. Result and Discussion

The system was designed to be used primarily in monitoring works of large engineering structures. Thus, it was tested in a dam 67 meters (220 ft) high, 1,100 meters (3,600 ft) long, that has a geodetic network built for monitoring purposes. The Salto Caxias Hydroelectric power plant is located between the municipalities of Capitão Leônidas Marques and Nova Prata do Iguaçu, 650 km far from Curitiba, Brazil (Figure 10).

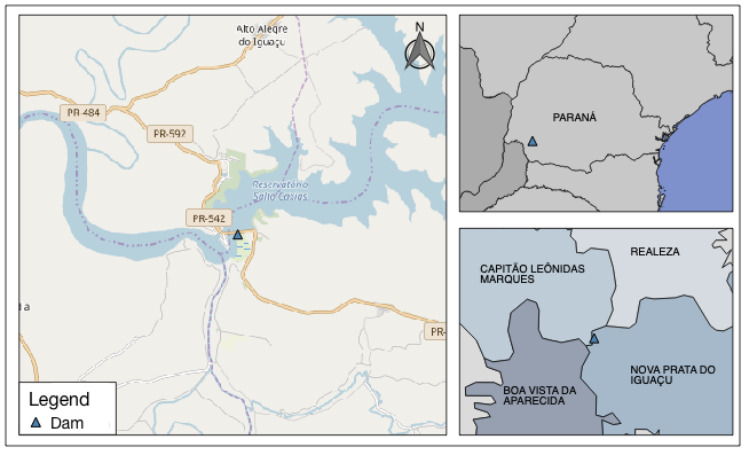

Figure 10. The location of Salto Caxias hydroelectric plant

In this dam there is an external monitoring network (Figure 11) composed of six forced centering pillars (fixed points) and several prisms fixed on the upstream face of the dam (object points). In addition, there is an internal monitoring network, used to measure points in the inspection-galleries of the dam

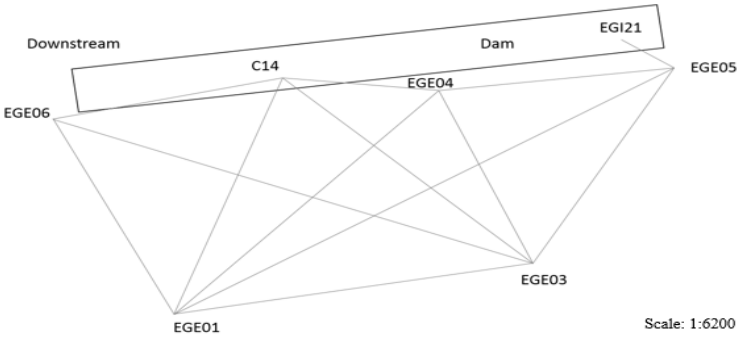

Figure 11. External control geodetic network

The observation of external network provides the geodetic control for the galleries. Figure 12, the position of the point EGE05 allows the connection of both networks through observation to the point EG21 that correspond to the inner geodesic station closest to the outside of the gallery. For this connection, the total station was set up at point EGE05 and is realized the back sight at point EGE04 (inclined distance of approximately 116 meters) and foresight at point EGI21 (approximately 37 meters).

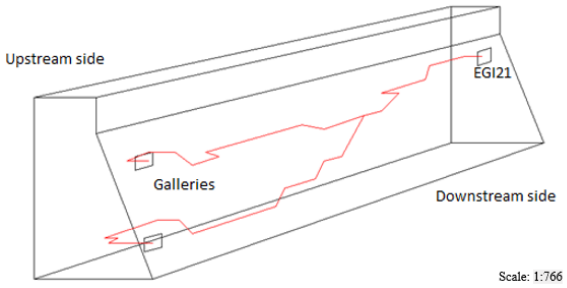

Figure 12. Gallery geodetic network, adapted (Zocollotii Filho, 2005)

The sensors were installed at the EGE04 point (sensor S5455), EGE05 (sensor S5451) and EGI21 (sensor S6579). Figure 13, 14 and 15 show the localization of the sensors

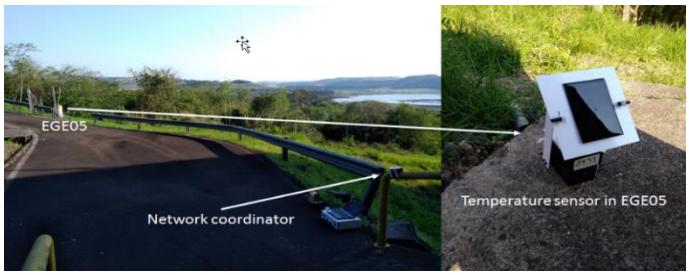

Figure 13. EGE05 temperature sensor installation

Figure 14. EGE04 temperature sensor installation

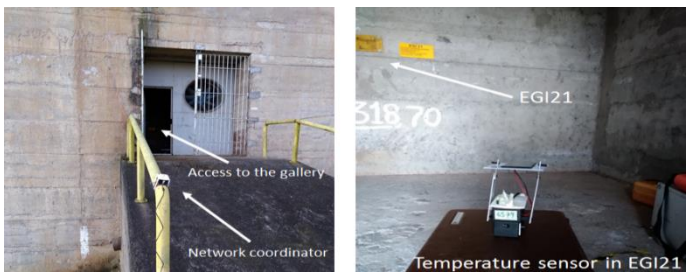

Figure 15. EGI21 temperature sensor installation

The sensors provided a temporal temperature series of two hours approximately. Figure 16 shows the temperature variations during the experiment.

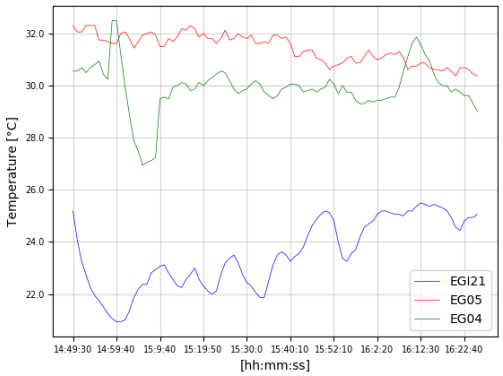

Figure 16. The temperature variation in EGI21, EGE05 and EGE04

This experiment seeks to present the behavior of the temperature around the dam. For this, in EGE03 pillar one sensor provides temperature at the total station position. Near the downstream prisms line, the other four sensors provided the temperature near these object points. These sensors were placed at different heights. Figure 17 shows the sensors distribution. The distance from the EGE03 point to the prisms and the sensors was approximately 280 meters.

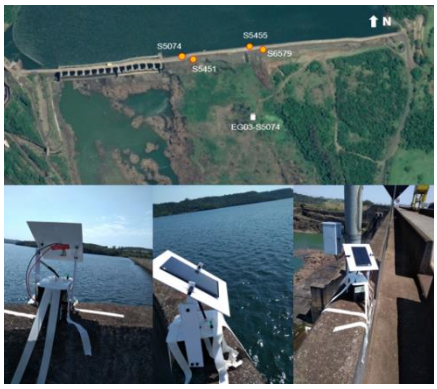

Figure 17. Sensors distribution in the dam for the second test

In this experiment, the five sensors provided a temporal series about 50 minutes of collected temperature values. Figure 18 shows the temperature variations during the experiment

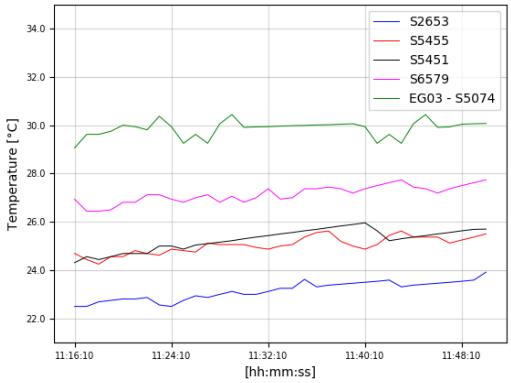

Figure 18. Temperature values of five sensors located in Salto Caxias dam

The Figure 18 show variations around 8°C between the different places where the temperature sensor was installed. An analysis was made comparing the precision of electronic distances and the refractive index, the last one was computed using the maximum difference of temperature during the second experiment (8°C). For the refractive index was used Equation 3, with pressure and humidity measured on where the total station was installed. For electronic distance precision was used the Equation 7

$$\sigma_D = \sqrt{(\sigma_i^2 + \sigma_t^2 + a^2 + (D \cdot b\ ppm)^2)} \tag{7}$$

Where σ_i^2 and σ_t^2 miscentering error for instrument and reflector respectively, a and b are specific accuracies and D is distance (Ghilani, 2017). To perform the analysis we choose a high precision electronic distance meter (1 + 0.5ppm) and the EGE03 – Dam distance (280m approximately). For the compute the distance precision, we inconsiderate miscentering error for instrument and reflector since both are fixed in the pillar for monitoring and in the body of dam respectively. Results are presented in Table 4.

Table 4. Comparison between index refraction and electronic distance precision

Approximate distance	Index refraction influence on distance (first velocity correction) (m)	distance precision (68% interval confidence) (m)
EGE03 – Dam (280m)	0.002	0.001

The results show that the variation in meters generated when considering the difference between the refractive indices is greater than the precision provided by the instrument for the distance used. Considering that the pressure and humidity parameters were considered fixed, the temperature and its variations affect the performance of the instrument.

For evaluation the influence of temperature on coordinate precision, we simulated a 2D topographic network (Figure 19) with two-control point (A, D), two unknown points (B, C) and five distances (continuous lines). To obtain the coordinates and their precisions we used trilateration technique and parametric least squared method (Ghilani, 2017). The refraction index was compute with the temperature data set from the acquisition system presented in the section 3.5 during the second experiment. With these values, we developed two mathematical models to temperature determination. In the first approach, we used the temperature value measured in the place where the total station was installed (classic approach), while that the second approach was obtained through the mean temperature value from the five sensors used in the previous experiment. For the pressure and humidity parameters, we used the values measured with external sensors on the total station position during the experiment presents in the section 4.1, for this simulation these parameters are considering invariants.

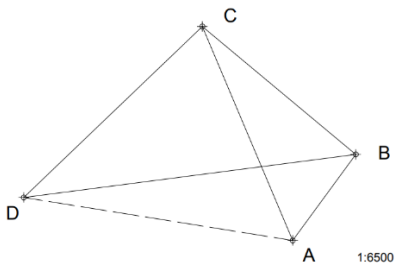

Figure 19. The simulated network

The refraction index values for the first and second approaches are 18.49 ppm and 17.38 ppm respectively. With these values, the first velocity and their distance precision were computed to each distance on the simulated network. The precision of B and C points are presented in Table 5:

Table 5. Precision coordinates B and C

Temperature approach	B (68% interval confidence)		C (68% interval confidence)	
	X (m)	Y (m)	X (m)	Y (m)
One sensor	0.0052	0.0086	0.0072	0.0054
Mean (5 sensors)	0.0049	0.0081	0.0068	0.0051

For the confidence interval used, the precisions reached through the use of an mean of temperature are better than those obtained in the traditional way. This may be because the second approach provides a more representative temperature value of the region.

For the first experiment, the temperature values presented differences in the EGI21, EGI21, EGI21 control points (maximum value of 12°C). These differences could be originated by different factors such as the temperature dissipated by the structure or environmental conditions around the dam. Both factors can create different thermal conditions in each control point, with irregular variations. In the geodetic monitoring context, the external network is used as reference for the displacement analysis of internal network, the latter, provides relevant information about the health of the structure. For the deformation analysis of internal network it is necessary the connection between networks, this is made through angles and distance measurement, consequently the temperature values provides by the developed system and the differences found should be considered in the distance measurement. In the second experiment, the temperature sensors were installed on the top and around the dam. Were collected temperature values during the geodetic monitoring of points on the downstream. The results show that temperature values decreasing with increasing the height, however the decreasing it is not regular. Some of the possible factors that influence the temperature values are the heat dissipation of the structure and the water mass influence on the points that are on the dam top. In both experiments, the temperature values have an irregular comportment during the geodetic monitoring. These variations can be affecting the correct determination of first velocity correction, thus the distances obtained by EDM.

The uncertainties generated by the temperature differences were obtained thought the first velocity correction, for this, the highest temperature difference found in these experiments (8°C) was used. This difference was obtained between the pillar EGE03 and a monitoring point on the top of the dam. The approximate distance between them is 280 meters and uncertainties are 2.0 mm approximately. The comparison between the uncertainties generated by the refractive index variations and the distance precision (1 mm) show that the temperature value is determinant to obtain precise distances by electromagnetic wave propagation.

For the coordinate precision values, the 2D simulate network show that the precisions of coordinates provide by the least square method are better where the refractive index was calculated with the mean temperature of sensors. Thus, the modeling of temperature is necessary for the geodetic monitoring of structures, where the correct determination of distances is relevant to the coordinate compute and deformation analysis.

4. Conclusion

The system development for temperature acquisition provides in real-time values in multiple locations. This characteristic permits temperature monitoring during the observation of a geodetic network or in other related activities. The temperature values obtained in the dam experience and their variations in different locations around to dam can affect the calculation of the first velocity correction. Considering that variation on 1°C affect distances in 1ppm and that it was found in both experiments, differences up to 8°C, to work in

temperature modeling for this correction is necessary. The experiments carried out show the importance of temperature both in determining distances and in coordinate precision of a topographic network, in this context, the developed system allows to collect data for modeling and provide a more representative temperature value.

5. Acknowledgments

The authors would like to thank Copel - Companhia Paranaense de Energia for allowing the tests to be carried out at the Salto Caxias plant. The authors also thank for the scholarship given.

6. References

Agresti, A. (2007). *An introduction to categorical data analysis*. John Wiley & Sons.

Angus-Leppan, P. V, & Brunner, F. K. (1980). Atmospheric temperature models for short-range EDM. *The Canadian Surveyor*, *34*(2), 153–165.

Artese, S., & Perrelli, M. (2018). Monitoring a landslide with high accuracy by total station: a DTM-based model to correct for the atmospheric effects. *Geosciences*, *8*(2), 46.

Brunner, F. K. (1984). Geodetic refraction. *Berlin: Shringer*, *216*.

Brunner, F. K., & Fraser, C. S. (1977). An atmospheric turbulent transfer model for EDM reduction. *Proc. IAG Symp., Wageningen*.

Brunner, F. K., & Rüeger, J. M. (1992). Theory of the local scale parameter method for EDM. *Bulletin Géodésique*, *66*(4), 355.

De Rubeis, T., Nardi, I., & Muttillo, M. (2017). Development of a low-cost temperature data monitoring. An upgrade for hot box apparatus. *Journal of Physics: Conference Series*, *923*(1), 12039.

Devices, A. (2020). Low voltage temperature sensors TMP35/TMP36/TMP37. *Analog Devices: Norwood, MA, USA*.

Fraser, C. S. (1981). A simple atmospheric model for electro-optical EDM reduction. *Australian Surveyor*, *30*(6), 352–362.

Ghilani, C. D. (2017). *Adjustment computations: spatial data analysis*. John Wiley & Sons.

Maxim, I. (2020). Programmable Resolution 1-Wire Digital Thermometer. *Data Sheet DS18B20*.

Ogundare, J. O. (2015). *Precision surveying: the principles and geomatics practice*. John Wiley & Sons.

Robertson, K. D. (1977). The use of atmospheric models with trilateration. *Survey Review*, *24*(186), 179–188.

Rüeger, J. M. (1990). *Electronic distance measurement: An introduction*. Springer Science & Business Media.

Scaioni, M., Barazzetti, L., Giussani, A., Previtali, M., Roncoroni, F., & Alba, M. I. (2014). Photogrammetric techniques for monitoring tunnel deformation. *Earth Science Informatics*, *7*(2), 83–95.

Soares, W. A. (2006). Investigação de uma modelagem matemática como alternativa para aumento da área de cobertura de estações de referência DGPS. *Boletim de Ciências Geodésicas*, *12*(1).

Solarić, N., Barković, DJuro, & Zrinjski, M. (2012). Automation of the Measurement of Atmospheric Parameters in Precise Distance Measurement. *Geodetski List*, *66*(3), 165–186.

Torge, W., & Müller, J. (2012). *Geodesy*. de Gruyter.

Ussisoo, I. (1969). Correction problems in electronic distance measurements. *Tellus*, *21*(4), 549–567.

Zocollotii Filho, C. A. (2005). Utilização de Técnicas de Poligonação de Precisão para o Monitoramento de Pontos Localizados em Galerias de Inspeção: Estudo de Caso da Usina Hidrelétrica de Salto Caxias. *Boletim de Ciências Geodésicas*, *11*(2), 287–288.